Annals of Biomedical Engineering, Vol. 39, No. 7, July 2011 *(© 2011)* pp. 1882–1890
DOI: 10.1007/s10439-011-0289-2

Electrospun Hydroxyapatite-Functionalized PLLA Scaffold: Potential Applications in Sternal Bone Healing

Alberto Rainer,[1] Cristiano Spadaccio,[2] Pietro Sedati,[3] Federico De Marco,[4] Simone Carotti,[5] Mario Lusini,[2] Gianluca Vadalà,[6] Alberto Di Martino,[6] Sergio Morini,[5] Massimo Chello,[2] Elvio Covino,[2] Vincenzo Denaro,[6] and Marcella Trombetta[1]

[1]Tissue Engineering Laboratory, Center for Integrated Research, University Campus Bio-Medico of Rome, via Álvaro del Portillo 21, 00128 Rome, Italy; [2]Area of Cardiovascular Surgery, Center for Integrated Research, University Campus Bio-Medico of Rome, via Álvaro del Portillo 200, Rome, Italy; [3]Area of Image Diagnostics, Center for Integrated Research, University Campus Bio-Medico of Rome, via Álvaro del Portillo 200, Rome, Italy; [4]Laboratory of Virology, Italian National Cancer Institute "Regina Elena", via delle Messi D'Oro 153, Rome, Italy; [5]Laboratory of Anatomy and Ultrastructural Microscopy, Center for Integrated Research, University Campus Bio-Medico of Rome, via Álvaro del Portillo 21, Rome, Italy; and [6]Area of Orthopaedics and Trauma Surgery, Center for Integrated Research, University Campus Bio-Medico of Rome, via Álvaro del Portillo 200, Rome, Italy

(Received 1 November 2010; accepted 2 March 2011; published online 15 March 2011)

Associate Editor K. A. Athanasiou oversaw the review of this article.

Abstract—Sternal synthesis after median sternotomy, a conventional access practice in thoracic and cardiac surgery, is at the basis of severe complications, often impairing the clinical outcome of surgical interventions. In this work, we propose the use of an acellular biomaterial scaffold, to be interposed across the fracture rime during closure operations, directly exposing the biomaterial to bone marrow, in order to expedite healing process. A rabbit model of median sternotomy was performed and an electrospun scaffold composed of a hydroxyapatite-loaded absorbable biopolymer (poly-L-lactide), shaped into a fibrillar structure, was used. CT follow-up confirmed a complete healing in the scaffold-treated group 1 week before the control. Histological evaluation demonstrated presence of newly formed bone *trabeculae* among scaffold fibers showing a higher degree of maturity with respect to the control untreated group. The proposed approach is able to both guide a more rapid healing and modulate inflammatory response across the wound site, resulting in improved healing and tissue remodeling with respect to conventional closure technique.

Keywords—Acellular scaffold, Poly(L-lactide), Hydroxyapatite, Electrospinning, Median sternotomy, Bone healing.

INTRODUCTION

Bone tissue engineering is emerging as a promising therapeutic tool in the clinical arena. Combining cells, biomaterials and biochemical regulatory signals, it pursues the repair and regeneration of diseased tissues and large structural defects.[17] In attempt to address the issues of reconstructive surgery following wide excisions of bone tumors or repair of complicated fractures, a number of strategies for bone tissue engineering have been developed in recent years.[9,31] Especially in pediatric departments, thoracic and cardiovascular surgeons face with major congenital chest wall defects posing significant morbidity and mortality to infants.[11] Repair is often hindered by lack of sufficient tissue available for surgical reconstruction, particularly in the neonatal period.[37,39] In this scenario, tissue engineering approach appears as one of the most effective strategies to restore anatomic continuity and tissue integrity.

In the current cardiothoracic surgery practice, standard access to mediastinal structures and organs requires a particular type of sternal fracture that, even if not constituting a major tissutal defect, is at the basis of several complications impairing clinical outcome and importantly affecting the overall cost of medical interventions.[7,20,42]

Median sternotomy, developed by Julian in 1957, is the preferred approach for cardiac surgery,[19] providing excellent exposure and wide surgical maneuvering

Address correspondence to Alberto Rainer, Tissue Engineering Laboratory, Center for Integrated Research, University Campus Bio-Medico of Rome, via Álvaro del Portillo 21, 00128 Rome, Italy. Electronic mail: a.rainer@unicampus.it

area, while the use of steel wires for sternal closure—firstly used by Milon (1944)—has been the standard approach for sternal resynthesis.[18] Anatomic and physical factors related with chest wall anatomy and closure procedures are thought to be among the mechanisms underlying the occurrence of sternal wound complications, including non-union, dehiscence, and infection,[38] which burden on 1–3% of patients undergoing cardiac surgery.[6,10,13,27]

Use of biomaterials might be a helpful approach in this context, which is characterized by limited and surgically controlled tissue loss, in order to promote cellular response and guide cell proliferation, eventually improving bone healing.

Indeed, scaffolds represent the pivotal structure of engineered tissue and establish a favorable environment for the synthesis of neo-extracellular matrix (ECM). The scaffold component is expected to support cell colonization, migration, growth and differentiation, guiding tissue development.[5] The addition of biologically active signals as ECM components or growth factors to this main backbone may have the potency to induce, support, or enhance the growth and differentiation of progenitor cells toward the desired lineage and to orchestrate tissue repair effectively.[41]

Several studies demonstrated that the ECM *milieu* surrounding cells has physical and structural features in the nanometer scale, and that this arrangement may affect several aspects of cell behavior such as morphology, adhesion, and cytoskeletal arrangements.[45,50,51] Thus, a great effort has been made to fabricate synthetic materials into nanometer scale structures in attempt to simulate the matrix environment.[15,30,34] Electrospinning is one of the approaches that allow the fabrication of synthetic materials into fibrous structures in the micro- and nanometer scale.[26,33]

Engineering of tissues rich in ECM components, such as cartilage and bone, normally benefits from an ample framework for cell attachment, which is a prerequisite for extracellular matrix synthesis, not to mention cell growth and differentiation. Fibers porosity is also a critical factor, promoting cell adhesion and engrafting. Similarly to native collagen, electrospun scaffolds feature high porosity (up to 90%) and mesh openings that range from a couple of microns to several hundreds.[24] All combined, these characteristics closely mimic the architectural scale and morphology of natural extracellular matrix.[4,8,48]

Poly(L-lactide) (PLLA) has been widely investigated because of its good biocompatibility[40,46,47] and the possibility to be modified with inorganic materials to improve its biological properties for tissue engineering purposes.[21,22,32,35] Among these, calcium phosphates—e.g., tricalcium phosphate (β-TCP) and hydroxyapatite (HA)—have been widely investigated, due to their similarity to the mineral component of natural bone, and considered osteoconductive materials allowing new bone formation.[2,14,23]

Recently, our group has developed a hydroxyapatite-functionalized electrospun PLLA scaffold with the aim to recapitulate the native histoarchitecture and molecular signaling of osteochondral tissue to facilitate the differentiation of stem cells seeded therein.[43] Here we test the ability of this previously characterized scaffold to promote bone repair in a rabbit model of median sternotomy, simply interposing the biomaterial at the fracture site. This model allowed to expose bone marrow, one of the most rich and advantageous sources of mesenchymal bone progenitors, enabling a direct interaction of the endogenous cells with a scaffold actively emanating a biological osteoinductive signaling.

MATERIALS AND METHODS

Scaffold Preparation and Characterization

The poly(L-lactide)/hydroxyapatite (PLLA/HA) nanocomposite was prepared by electrospinning technique, starting from a dispersion of HA nanopowder in a PLLA solution as we have recently reported.[43] Briefly, 1 g of PLLA (inherent viscosity 0.90–1.20 dL/g, Sigma) was dissolved in 5 mL of dichloromethane (Sigma), and 0.1 g nanosized HA powder (particle size < 200 nm, Sigma) was dispersed in the polymer solution under stirring. An electrospinning apparatus was used (Dynaspin, Biomatica). The obtained suspension was transferred into a glass syringe, actuated by an infusion pump (1.5 mL/h) and fed through a 23G needle, which was kept at a high DC voltage (15 kV) with respect to an earthed target facing the needle at a distance of 15 cm.

Microstructure of the obtained membranes was evaluated by Field Emission Scanning Electron Microscopy (FE-SEM, Leo Supra 1535, Leo Electron Microscopy). Prior to implantation, PLLA/HA patches were sterilized by hydrogen peroxide gas plasma (ASP Sterrad).[29]

Median Sternotomy Model

A total of 12 male New Zealand rabbits, weighing 3.5 ± 0.5 kg (Charles River Laboratories) were used for this study. Six animals were used for treatment with PLLA/HA scaffold following median sternotomy, and six for sham controls.[44]

Animals were housed one rabbit per cage in an animal research facility (Regina Elena Institute, Rome). The facility maintains an environment of

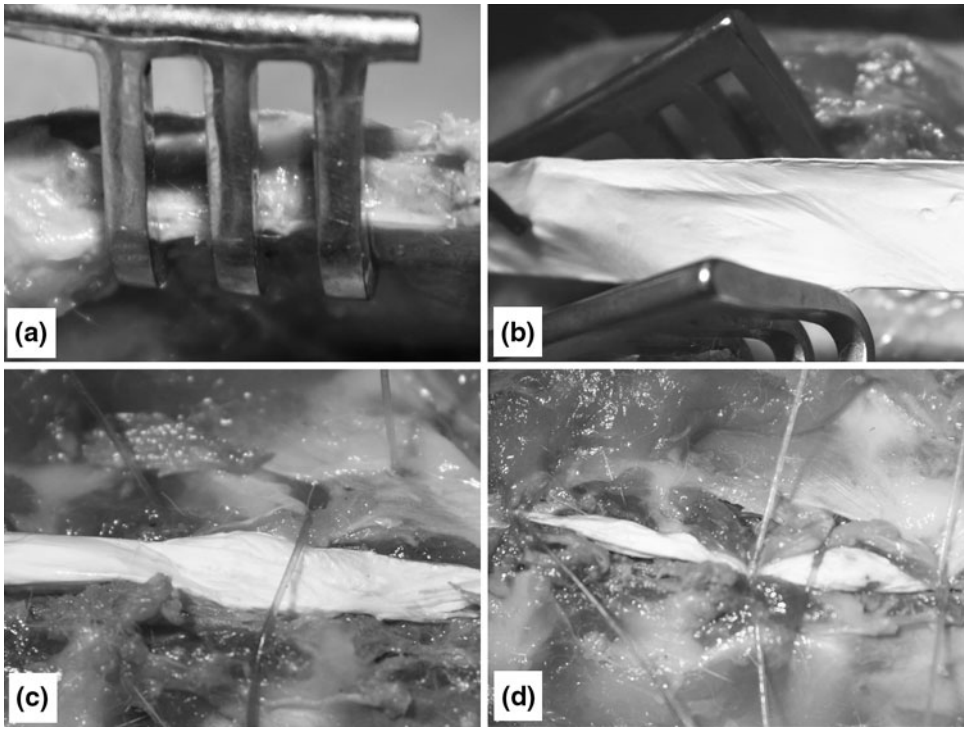

FIGURE 1. Intraoperative images. (a) Detail of the fracture rime after median sternotomy; (b) interposition of the biomaterial scaffold; (c, d) closure with intercostal wires.

controlled temperature, with a 12 h light/dark cycle. Rabbits were supplied with sterile bedding, standard food and water, and were acclimatized for 10 days before each experiment. Animals were individually labeled and weighed prior to each experiment, and were humanely sacrificed by carbon dioxide at its termination. All procedures, care and handling of the animals were reviewed and approved by the Institutional Animal Care and Use Committee at Regina Elena Institute, Rome.

Prior to surgery, rabbits were anesthetized with a 2:1 mixture of ketamine-HCl (100 mg/ml):xylazine (20 mg/ml) at a dose of 0.75 ml/kg im. A 20-gauge intravenous catheter was placed in a marginal ear vein for intravenous access. Each animal was secured in a supine position and chest was clipped and prepared for the operation with povidone–iodine and ethyl alcohol. Hypothermia was prevented with a surgical warming pad, and lactated Ringer's solution was infused through the intravenous catheter at 5–15 mL/h. Following a midline skin incision, both *pectoralis major* muscles were dissected and divided on the medial border from the insertion to the sternum, leaving the sternal bone well exposed. An incision was performed using a circular saw, leaving similar parts of the sternum on both sides (Fig. 1a). Meticulous hemostasis was achieved using sterile sponges. In the control group ($n = 6$), sternum was closed with 3.0 absorbable cut gut wires by means of figure-8 technique. In the study group ($n = 6$), length of the fracture line was measured and an adequate layer of PLLA/HA electrospun scaffold was interposed between the two sternum halves (Fig. 1b). Sternum was then closed using cut gut wire in the same figure-8 fashion (Figs. 1c, 1d). Acetaminophen (0.25 mg/mL) in the drinking water was used as a post-operative analgesic.

Computed Tomography (CT)

CT follow-up evaluation was performed on all animals that had undergone surgery at regular timepoints (1, 2, 3, and 4 weeks). Animals were properly sedated by midazolam at a dose of 2 mg/kg im, recommended as a short-acting sedative drug for diagnostic procedures.[36]

All CT examinations were performed on a SOMATOM Sensation 64 CT scanner (Siemens Medical Solutions) with a 32 × 0.6 mm detector configuration, capable of acquiring 64 × 0.6 mm slices by applying the *z*-axis flying focus technique.[12]

Primary axial reconstructions were performed with a slice thickness of 0.75 mm and a reconstruction increment of 0.5 mm. Field of view was adapted to the sternum size (FOV 50 mm), and a convolution kernel dedicated to bone was adopted. All datasets gathered by multidetector CT were transferred on a dedicated

workstation (Leonardo, Siemens Medical Solutions) for analysis.

In order to properly orientate reconstructions along anatomical directions, oblique multiplanar reconstructions (MPRs) were obtained from each dataset rearranging the axes along sternum orientation.

Bone density (BD) was calculated, in terms of Hounsfield units (HU), on axial reformatted images (perpendicular to the long axis of the sternum) using a circular region of interest (ROI).[49] Positioning of slices and ROIs was standardized throughout the follow-up. For the present study, five representative slices, equally spaced within the median third of the second metamer were chosen for each animal. For each slice, five circular ROIs (with an area of 2 mm^2), were placed along the fracture rime. BD was determined by calculating the average of HU values gathered from all ROI measurements. Data were processed using SPSS (Statistical Package for Social Sciences) release 13.0 for Windows. Data are presented as mean ± SD. One-way ANOVA was performed to compare groups at each timepoint, followed by multiple pairwise comparisons procedure (Tukey test). Assumptions of normality were checked and met. Pearson's product-moment r coefficient was calculated to evaluate correlations. Significance was at the 0.01 level.

Sternal Repair Evaluation

After 4 weeks, animals were sacrificed and sternal bone explanted for histological evaluation. For each animal, contiguous cross-sections of the metamer undergone CT evaluation were immediately fixed in 10% formaldehyde solution and, after accelerated decalcification process,[16] samples were cut and stained for standard hematoxylin-eosin (Sigma) staining and evaluated by light microscopy (Olympus BX-51). Reconstruction of the whole sternum was performed through a dedicated image acquisition software (Delta Sistemi), featuring a dedicated merge module.

RESULTS

Scaffold Microstructural Evaluation

Figure 2 shows the results of FE-SEM observations on PLLA/HA scaffold. The material appeared as a nonwoven mat with an approximate thickness of 300 μm, composed of micron-sized fibers (average diameter 3.5 ± 0.9 μm). At higher magnification, a dispersion of HA nanoparticles (particle size < 200 nm) was detected on the surface of PLLA fibers. Moreover, fibers surface showed an intrinsic porosity with an average pore size of approximately 100 nm.

Computed Tomography (CT)

A representative reconstruction of the whole rabbit sternum undergone median sternotomy—illustrating the features of the anatomical site—is reported in Fig. 3a. In the same panel, the reconstruction of a portion of the sternum after surgery is shown for the PLLA/HA group (Fig. 3b) and for the control (Fig. 3c).

Figure 4 reports axial reformatted images for treated and control groups at different timepoints. Bone density (BD) was calculated at each timepoint and results are plotted in Fig. 5.

At each timepoint, mineral density in the PLLA/HA group was found to be significantly higher than the control group ($p < 0.01$). Interestingly, an accurate analysis of the evolution of BD over time showed values peaking significantly earlier in the PLLA/HA group than in the control, and slightly reaching a plateau at 4 weeks following operation.

As shown in Fig. 4, a complete healing of sternal fracture was observed 21 days after surgery in the treated group, while in the control group a definite fracture rime could still be observed at the same timepoint. Additionally, at weeks 2 and 3, the perilesional zone in the control group was characterized by a fuzzy hyperdensity (straight arrows), which could be reasonably ascribed to high cellularity, compatible with an

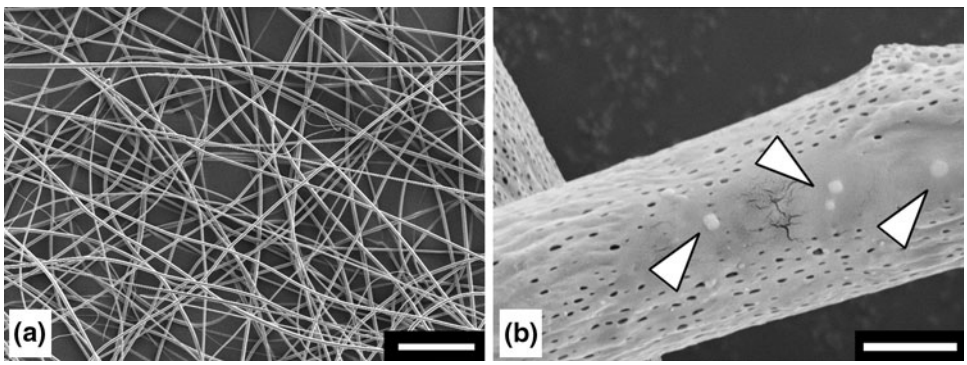

FIGURE 2. Scaffold microstructure. FE-SEM micrographs of the scaffold at different magnifications. (a) Scale bar: 50 μm. (b) Scale bar: 2 μm; arrows indicate hydroxyapatite nanoparticles on the surface of PLLA fibers.

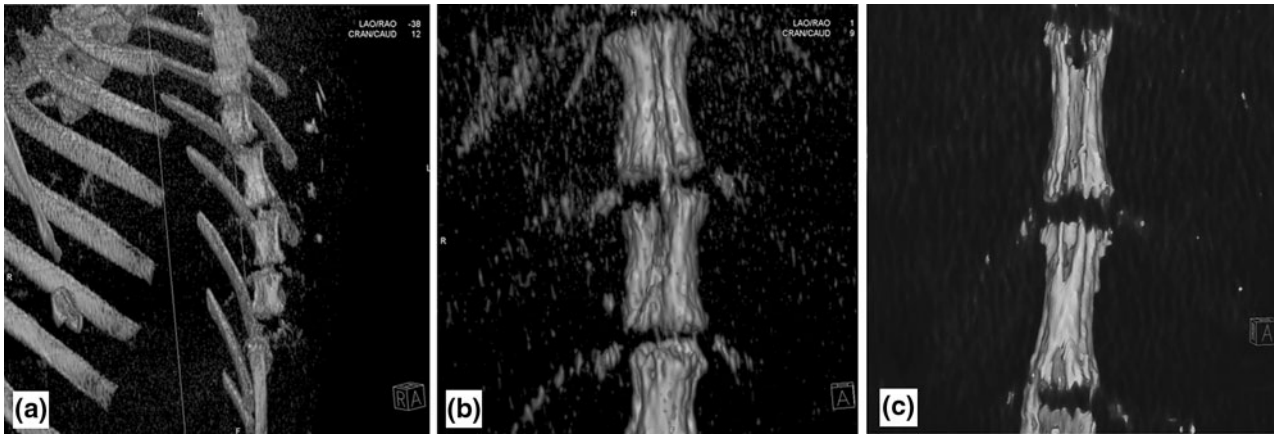

FIGURE 3. CT reconstruction of the sternum. (a) CT reconstruction at 1 week for an animal in the PLLA/HA group is reported; a higher magnification detail of the fractured metamers is reported for the PLLA/HA (b) and control (c) groups.

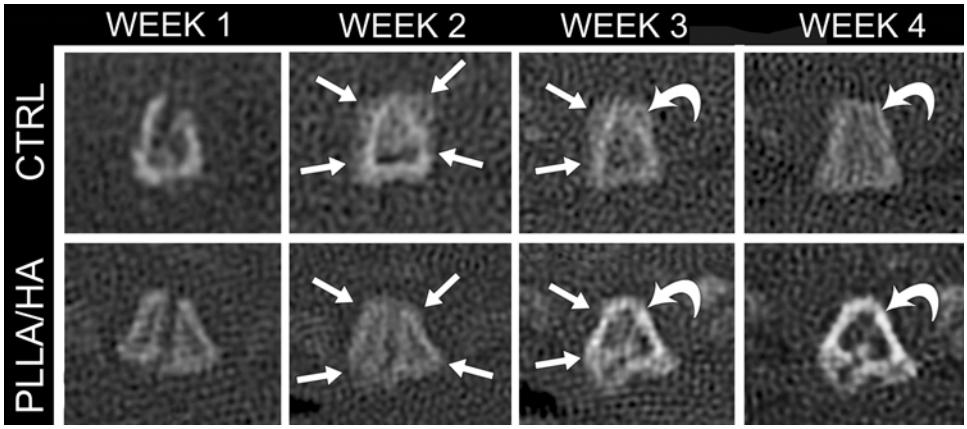

FIGURE 4. CT follow-up. Reformatted axial scans of a given sternum metamer for the treated and control groups at different timepoints. Straight white arrows delineate a fuzzy hyperdensity in the pericortical bone tissue in the control group that is not visible in the PLLA/HA group. Curved arrows indicate a higher degree of separation between cortical and spongious bone in the PLLA/HA group, which is not evidenced in the control group.

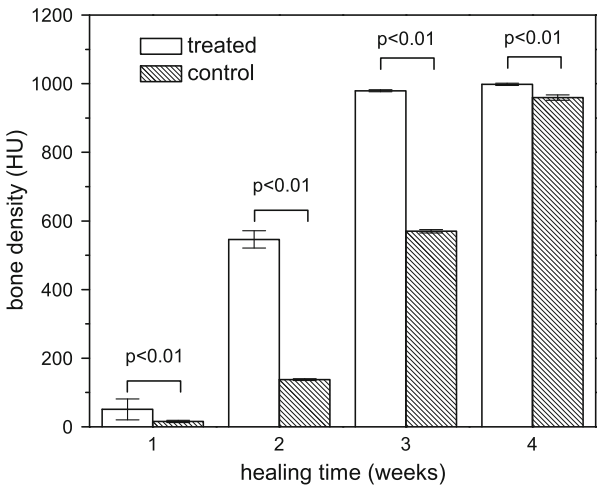

FIGURE 5. Bone density measurements. Bone density values (expressed in Hounsfield units) measured at selected timepoints for treated and control groups.

inflammatory process. This observation couples with the finding of a non-adequate alignment of sternal halves in the control. These findings were not observed in the PLLA/HA group, in which a significantly less hypertrophic callus formation could be described. Interestingly, at 4 weeks CT scans of the PLLA/HA group showed an advanced state of bone remodeling resulting in a clear separation and definition of the outer cortical zone with respect to the inner cancellous bone (curved arrows), that was not observed in the control. Bone repair in the PLLA/HA group approximated healthy findings of non-damaged controls. This might reliably indicate a more mature phase of bone healing.

Histological Analysis

Results of histological analysis of segments from treated and control groups after 4 weeks from surgery are shown in Fig. 6.

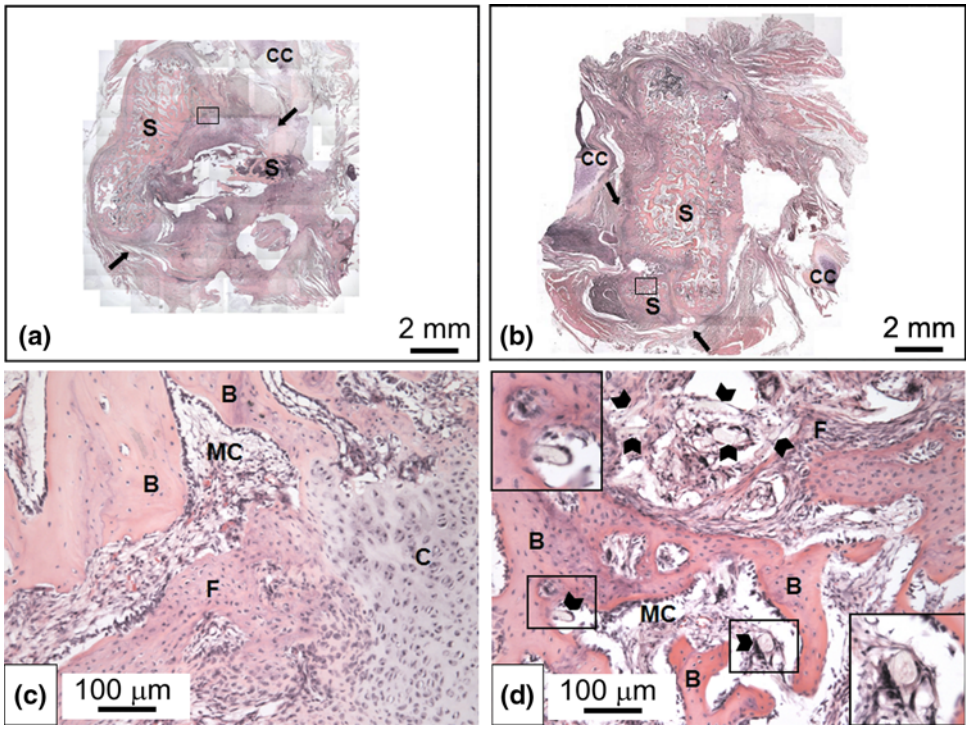

FIGURE 6. Histological evaluation. Upper panel shows representative reconstruction of the entire sternum (S) with partially preserved costal cartilage (CC) 4 weeks after surgery in the control (a) and experimental group (b). Black arrows identify direction of the fracture rime. In the lower panel, magnified fields taken near the fracture area are shown (c, d). Although bone defects in the two groups underwent a similar reparative process, the amount of bone formation and the degree of maturity were significantly lower in the control group (a, c) compared to those in the experimental group (b, d). In the control group (a, c) islands of cartilage (C) and fibrotic tissue (F) as result of the healing process at the bone defect site could be observed, while the experimental group showed large amount of newly formed trabecular bone (B) with a milder degree of fibrosis (b, d). According to the radiological findings of a higher degree of bone organization with a clear separation of cortical and spongious bone, histological correlate in the experimental group shows forming marrow cavities (MC) adjacent to the bone *trabeculae* (d). Arrowheads (d) indicate scaffold residuals. a, b: Original magnification ×40; calibration bar 2 mm. c, d: Original magnification ×100; calibration bar 100 μm. High power fields: original magnification ×200.

PLLA/HA group showed new bone formation, as evidenced by regenerated bone *trabeculae* and normal bone marrow structure with reduced fibrosis. All PLLA/HA implants showed evidence of a good engraftment, displaying typical bone morphology. Scaffold residuals could be detected in the forming marrow cavities (arrowheads in Fig. 6d). Despite the foreign origin of the scaffold material, only very few scattered mononuclear infiltrates were noted in some samples. Evidence of active bone remodeling was frequently found at the periphery of the grafts with the polymer being almost completely absorbed. These findings are consistent with an advanced healing process in the PLLA/HA group.

Although bone defects in the control group underwent a similar reparative process, the amount of bone formation and the degree of maturity were significantly lower compared to PLLA/HA group. In contrast, analysis of the control segments showed intense inflammatory reaction at the fracture site with high cellularity and dense lympho-monocytic infiltration accompanying bone repair. In the control group, islands of cartilage and fibrosis were more present compared to PLLA/HA group. Additionally, some segments appeared to be healed with fibrotic scarring, with little evidence of new bone formation.

DISCUSSION

In conventional sternum closure procedures, the only cohesive force acting upon reunited sternum in the initial early postoperative period is the holding force of sternal sutures. This is determined by several factors, as number and location of sutures, suture tightness, and exerted stress. If wires cut into the sternum after they are tied, sutures will loosen, the sternum halves will first moderately separate, and then, due to respiratory motion of the chest wall, the loose wires will literally cut the sternum into segments.[28] Despite current improvements in operative techniques, anesthesia, and antibiotic treatments, sternal dehiscence and mediastinitis, arising from uncomplete repair, are among the most severe complications of

median sternotomy, remaining a significant source of mortality and morbidity,[7,20,42] especially in the presence of predisposing factors determining poor bone quality as old age, osteoporosis, diabetes, obesity, steroid treatment, reoperation, early postoperative resuscitation, and use of bilateral thoracic arteries.[18] In this scenario, characterized by limited and controlled tissue loss, the use of biomaterials could be a valid alternative to promote and improve bone repair.

In a previous study, the Authors developed a hydroxyapatite-functionalized scaffold by means of electrospinning with the aim to recapitulate native histoarchitecture and molecular signaling of osteochondral tissue, to facilitate the differentiation of bone marrow-derived mesenchymal stem cells toward bony phenotypes. In that study, we demonstrated the ability of electrospun PLLA/HA fibers to exert an effective biological signaling resulting in the reorganization of the intracellular machinery with the final achievement of different phenotype.[43] Ultrastructural analysis of the scaffold also revealed an adequate porosity to favor cell attachment. Mesh openings matched the required dimensions reported in early studies in which the minimum requirement for pore size was considered to be approximately 50–100 μm, due to cell size, migration requirements, and transport.[17] These data represent a proof of principle of the possibility to produce a scaffold suitable for stem cells seeding, containing the appropriate factors to induce a guided differentiation towards the desired phenotype within a three-dimensional ECM-like environment closely mimicking the tissue native architecture. In the present work, we decided to test the *in vivo* ability of our previously developed functionalized scaffold to promote bone repair in a rabbit model of median sternotomy, simply interposing the biomaterial at the fracture site. In the proposed model, the role of the scaffold is not to fill important losses of substance; on the contrary, here the scaffold is intended as a guide for tissue restoration and regeneration. Noteworthy, the PLLA/HA nonwoven fabric—by virtue of its reduced thickness and high flexibility—demonstrated to easily adapt to the geometry of the lesion, following the profile of the fracture rime, and allowing for an optimal closure, without altering the geometrical features of the sternum.

Histological evaluation demonstrated presence of newly formed bone *trabeculae* among the scaffold fibers, showing a higher degree of maturity with respect to the control untreated group.

Differently from other approaches, in this study we did not pre-seed scaffolds with autologous stem cells.[44] According to a translational approach, cell-based therapies still need to overcome many hurdles for their actual clinical application, mainly regarding biological, economical, logistic, and ethical concerns. On the opposite, we focused on the optimization of biomimetic design of the scaffold and its differentiating abilities. The rationale underlying this study concerned the possibility to exploit endogenous reparative capabilities of the body and to guide these regenerative resources toward tissue restoration by means of a tailored absorbable material.

This model allowed to expose bone marrow, one of the most rich and advantageous sources of stem cells, enabling a direct interaction of the endogenous cells with a scaffold actively emanating a biological osteoinductive signaling.

Mimicking the ECM histoarchitecture, the scaffold provided at the same time a biological and mechanical support during the healing process, exerting a modulatory effect on cell colonization and orchestrating the body regenerative response in a regulated manner. Noteworthy, our findings are consistent with a more controlled and modulated tissutal reaction in the study group, as if biological signaling arising from the scaffold could mitigate the host response reducing the intensity of the inflammatory phase of the healing process (as confirmed by both radiological and histological observations) and orientate cellular reaction toward effective regeneration. The biomimesis principle inspiring the structure of this scaffold along with its functionalization with bioactive moieties, could therefore guide reparative processes and modulate damaged tissue microenvironment, favoring a regenerative drive over the inflammatory reaction. PLLA/HA scaffold was in the most part absorbed. As for other aliphatic polyesters, such degradation process can be attributed to hydrolysis of the ester bond,[25] which can be catalyzed by common enzymes naturally present in body fluids.[3] Interestingly, only mild signs of inflammatory response could be noticed in the study group, indicating a relative biocompatibility of the biomaterials.

The idea of an off-the-shelf available biomaterial to be promptly used to aid and hasten reparative processes of sternal fractures enabling a more rapid clinical recover of the patients could be interesting. Considering the current limitations hampering the use of cell therapy in regenerative medicine, an approach circumventing the use of cell-seeded constructs could expedite the clinical application of this exciting therapeutic resource.

Among limitations of this study, authors acknowledge the lack of histological analysis at multiple timepoints. However, in consideration of the possibility to appropriately evaluate major outcomes of this study by means of instrumental analysis and by virtue of the reported diagnostic accuracy of radiological imaging in sternal healing,[1] healing process was

accurately followed during time by CT scanning, allowing direct measurements of mineralization and fracture rime closure.

CONCLUSIONS

In this study we demonstrated the successful repair of median sternotomy in an animal model using a previously developed PLLA/HA scaffold. Differently from other models of sternal tissue engineering, our approach did not consider the use of autologous cells which would represent an additional limit in terms of clinical application. Here, we propose the development of a cell-free system able to exploit and boost endogenous repair and stem cell resources, guiding them towards tissue restoration. The idea of an off-the-shelf available biomaterial to be promptly used to aid and hasten repair of sternal fractures, reducing the overall sternal healing time, could be an important advance in the clinical management of patients undergoing cardiac surgery, as it could enable a more rapid recover and a dramatic reduction in the clinical *sequelae*. Additionally, this system would be able to circumvent the use of autologous cell transplantation, dramatically reducing costs, logistics, and time related to a cell-based approach.

ACKNOWLEDGMENTS

Authors would like to thank Giuseppe Bertini for his technical expertise in animal surgery.

CONFLICT OF INTEREST

The authors declare no conflict of interest.

REFERENCES

[1]Alkadhi, H., S. Wildermuth, B. Marincek, and T. Boehm. Accuracy and time efficiency for the detection of thoracic cage fractures: volume rendering compared with transverse computed tomography images. *J. Comput. Assist. Tomogr.* 28:378–385, 2004.

[2]Auclair-Daigle, C., M. N. Bureau, J. G. Legoux, and L. Yahia. Bioactive hydroxyapatite coatings on polymer composites for orthopedic implants. *J. Biomed. Mater. Res. A* 73:398–408, 2005.

[3]Azevedo, H. S., and R. L. Reis. Understanding the enzymatic degradation of biodegradable polymers and strategies to control their degradation rate. In: Biodegradable Systems in Tissue Engineering and Regenerative Medicine, edited by R. L. Reis, and J. San Román. Boca Raton, FL: CRC Press, 2005, pp. 178–201.

[4]Barnes, C. P., S. A. Sell, E. D. Boland, D. G. Simpson, and G. L. Bowlin. Nanofiber technology: designing the next generation of tissue engineering scaffolds. *Adv. Drug. Deliv. Rev.* 59:1413–1433, 2007.

[5]Bonzani, I. C., J. H. George, and M. M. Stevens. Novel materials for bone and cartilage regeneration. *Curr. Opin. Chem. Biol.* 10:568–575, 2006.

[6]Borger, M. A., V. Rao, R. D. Weisel, J. Ivanov, G. Cohen, H. E. Scully, and T. E. David. Deep sternal wound infection: risk factors and outcomes. *Ann. Thorac. Surg.* 65:1050–1056, 1998.

[7]Bottio, T., G. Rizzoli, V. Vida, D. Casarotto, and G. Gerosa. Double crisscross sternal wiring and chest wound infections: a prospective randomized study. *J. Thorac. Cardiovasc. Surg.* 126:1352–1356, 2003.

[8]Christenson, E. M., K. S. Anseth, J. J. van den Beucken, C. K. Chan, B. Ercan, J. A. Jansen, C. T. Laurencin, W. J. Li, R. Murugan, L. S. Nair, S. Ramakrishna, R. S. Tuan, T. J. Webster, and A. G. Mikos. Nanobiomaterial applications in orthopedics. *J. Orthop. Res.* 25:11–22, 2007.

[9]Donati, D., M. Colangeli, S. Colangeli, C. Di Bella, and M. Mercuri. Allograft-prosthetic composite in the proximal tibia after bone tumor resection. *Clin. Orthop. Relat. Res.* 466:459–465, 2008.

[10]Ehrenkranz, N. J., and S. J. Pfaff. Mediastinitis complicating cardiac operations: evidence of postoperative causation. *Rev. Infect. Dis.* 13:803–814, 1991.

[11]Engum, S. A. Embryology, sternal clefts, ectopia cordis, and Cantrell's pentalogy. *Semin. Pediatr. Surg.* 17:154–160, 2008.

[12]Flohr, T. G., K. Stierstorfer, S. Ulzheimer, H. Bruder, A. N. Primak, and C. H. McCollough. Image reconstruction and image quality evaluation for a 64-slice CT scanner with z-flying focal spot. *Med. Phys.* 32:2536–2547, 2005.

[13]Gardlund, B., C. Y. Bitkover, and J. Vaage. Postoperative mediastinitis in cardiac surgery—microbiology and pathogenesis. *Eur. J. Cardiothorac. Surg.* 21:825–830, 2002.

[14]Gomez-Vega, J. M., E. Saiz, A. P. Tomsia, G. W. Marshall, and S. J. Marshall. Bioactive glass coatings with hydroxyapatite and bioglass particles on Ti-based implants. 1. Processing. *Biomaterials* 21:105–111, 2000.

[15]He, W., T. Yong, Z. W. Ma, R. Inai, W. E. Teo, and S. Ramakrishna. Biodegradable polymer nanofiber mesh to maintain functions of endothelial cells. *Tissue Eng.* 12: 2457–2466, 2006.

[16]Hoole, P. F. Rapid decalcification of bone for diagnostic histology. *Med. Lab. Technol.* 28:201–204, 1971.

[17]Hutmacher, D. W., J. T. Schantz, C. X. Lam, K. C. Tan, and T. C. Lim. State of the art and future directions of scaffold-based bone engineering from a biomaterials perspective. *J. Tissue Eng. Regen. Med.* 1:245–260, 2007.

[18]Imren, Y., H. Selek, H. Zor, H. Bayram, E. Ereren, I. Tasoglu, and Y. Sariguney. The management of complicated sternal dehiscence following open heart surgery. *Heart Surg. Forum* 9:E871–E875, 2006.

[19]Julian, O. C., M. Lopez-Belio, W. S. Dye, H. Javid, and W. J. Grove. The median sternal incision in intracardiac surgery with extracorporeal circulation; a general evaluation of its use in heart surgery. *Surgery* 42:753–761, 1957.

[20]Karra, R., L. McDermott, S. Connelly, P. Smith, D. J. Sexton, and K. S. Kaye. Risk factors for 1-year mortality after postoperative mediastinitis. *J. Thorac. Cardiovasc. Surg.* 132:537–543, 2006.

[21]Kikuchi, M., Y. Koyama, K. Takakuda, H. Miyairi, N. Shirahama, and J. Tanaka. In vitro change in mechanical

strength of beta-tricalcium phosphate/copolymerized poly-L-lactide composites and their application for guided bone regeneration. *J. Biomed. Mater. Res.* 62:265–272, 2002.
[22]Kikuchi, M., Y. Koyama, T. Yamada, Y. Imamura, T. Okada, N. Shirahama, K. Akita, K. Takakuda, and J. Tanaka. Development of guided bone regeneration membrane composed of beta-tricalcium phosphate and poly (L-lactide-co-glycolide-co-epsilon-caprolactone) composites. *Biomaterials* 25:5979–5986, 2004.
[23]Lee, T. M., C. Y. Yang, E. Chang, and R. S. Tsai. Comparison of plasma-sprayed hydroxyapatite coatings and zirconia-reinforced hydroxyapatite composite coatings: in vivo study. *J. Biomed. Mater. Res. A* 71:652–660, 2004.
[24]Li, W. J., C. T. Laurencin, E. J. Caterson, R. S. Tuan, and F. K. Ko. Electrospun nanofibrous structure: a novel scaffold for tissue engineering. *J. Biomed. Mater. Res.* 60:613–621, 2002.
[25]Li, S., and M. Vert. Biodegradation of aliphatic polyesters. In: Degradable Polymers. Principles and Applications, edited by G. Scott. Dordrecht, The Netherlands: Kluwer Academic Publishers, 2003, pp. 71–132.
[26]Liu, Y., S. Sagi, R. Chandrasekar, L. Zhang, N. E. Hedin, and H. Fong. Preparation and characterization of electrospun SiO_2 nanofibers. *J. Nanosci. Nanotechnol.* 8:1528–1536, 2008.
[27]Loop, F. D., B. W. Lytle, D. M. Cosgrove, S. Mahfood, M. C. McHenry, M. Goormastic, R. W. Stewart, L. A. Golding, and P. C. Taylor. J. Maxwell Chamberlain memorial paper. Sternal wound complications after isolated coronary artery bypass grafting: early and late mortality, morbidity, and cost of care. *Ann. Thorac. Surg* 49:179–186, 1990; (discussion 186-177).
[28]Losanoff, J. E., A. D. Collier, C. C. Wagner-Mann, B. W. Richman, H. Huff, F. Hsieh, A. Diaz-Arias, and J. W. Jones. Biomechanical comparison of median sternotomy closures. *Ann. Thorac. Surg.* 77:203–209, 2004.
[29]Luong-Van, E., L. Grondahl, K. N. Chua, K. W. Leong, V. Nurcombe, and S. M. Cool. Controlled release of heparin from poly(epsilon-caprolactone) electrospun fibers. *Biomaterials* 27:2042–2050, 2006.
[30]Ma, Z., W. He, T. Yong, and S. Ramakrishna. Grafting of gelatin on electrospun poly(caprolactone) nanofibers to improve endothelial cell spreading and proliferation and to control cell orientation. *Tissue Eng.* 11:1149–1158, 2005.
[31]Mazurkiewicz, T., and M. Mazurkiewicz. Methods of reconstruction of large bone defects after tumor resection. *Ortop. Traumatol. Rehabil.* 7:465–469, 2005.
[32]Montjovent, M. O., L. Mathieu, B. Hinz, L. L. Applegate, P. E. Bourban, P. Y. Zambelli, J. A. Manson, and D. P. Pioletti. Biocompatibility of bioresorbable poly(L-lactic acid) composite scaffolds obtained by supercritical gas foaming with human fetal bone cells. *Tissue Eng.* 11:1640–1649, 2005.
[33]Nair, L. S., S. Bhattacharyya, and C. T. Laurencin. Development of novel tissue engineering scaffolds via electrospinning. *Expert Opin. Biol. Ther.* 4:659–668, 2004.
[34]Noh, H. K., S. W. Lee, J. M. Kim, J. E. Oh, K. H. Kim, C. P. Chung, S. C. Choi, W. H. Park, and B. M. Min. Electrospinning of chitin nanofibers: degradation behavior and cellular response to normal human keratinocytes and fibroblasts. *Biomaterials* 27:3934–3944, 2006.
[35]Oh, T., M. M. Rahman, J. H. Lim, M. S. Park, D. Y. Kim, J. H. Yoon, W. H. Kim, M. Kikuchi, J. Tanaka, Y. Koyama, and O. K. Kweon. Guided bone regeneration with beta-tricalcium phosphate and poly L-lactide-co-glycolide-co-epsilon-caprolactone membrane in partial defects of canine humerus. *J. Vet. Sci.* 7:73–77, 2006.
[36]Ramer, J. C., J. Paul-Murphy, and K. G. Benson. Evaluating and stabilizing critically ill rabbits. Part II. *Comp. Cont. Educ. Pract* 21:116–125, 1999.
[37]Samir, K., O. Ghez, D. Metras, and B. Kreitmann. Ectopia cordis, a successful single stage thoracoabdominal repair. *Interact. Cardiovasc. Thorac. Surg.* 2:611–613, 2003.
[38]Schimmer, C., S. P. Sommer, M. Bensch, T. Bohrer, I. Aleksic, and R. Leyh. Sternal closure techniques and postoperative sternal wound complications in elderly patients. *Eur. J. Cardiothorac. Surg.* 34:132–138, 2008.
[39]Shamberger, R. C. Congenital chest wall deformities. *Curr. Probl. Surg.* 33:469–542, 1996.
[40]Simon, C. G., Jr., N. Eidelman, S. B. Kennedy, A. Sehgal, C. A. Khatri, and N. R. Washburn. Combinatorial screening of cell proliferation on poly(L-lactic acid)/poly(D, L-lactic acid) blends. *Biomaterials* 26:6906–6915, 2005.
[41]Sohier, J., L. Moroni, C. V. Blitterswijk, K. D. Groot, and J. Bezemer. Critical factors in the design of growth factor releasing scaffolds for cartilage tissue engineering. *Expert Opin. Drug. Deliv.* 5:543–566, 2008.
[42]Song, D. H., R. F. Lohman, J. D. Renucci, V. Jeevanandam, and J. Raman. Primary sternal plating in high-risk patients prevents mediastinitis. *Eur. J. Cardiothorac. Surg.* 26:367–372, 2004.
[43]Spadaccio, C., A. Rainer, M. Trombetta, G. Vadala, M. Chello, E. Covino, V. Denaro, Y. Toyoda, and J. A. Genovese. Poly-L-lactic acid/hydroxyapatite electrospun nanocomposites induce chondrogenic differentiation of human MSC. *Ann. Biomed. Eng.* 37:1376–1389, 2009.
[44]Steigman, S. A., A. Ahmed, R. M. Shanti, R. S. Tuan, C. Valim, and D. O. Fauza. Sternal repair with bone grafts engineered from amniotic mesenchymal stem cells. *J. Pediatr. Surg.* 44:1120–1126, 2009; (discussion 1126).
[45]Stevens, M. M., and J. H. George. Exploring and engineering the cell surface interface. *Science* 310:1135–1138, 2005.
[46]Su, S. H., K. T. Nguyen, P. Satasiya, P. E. Greilich, L. Tang, and R. C. Eberhart. Curcumin impregnation improves the mechanical properties and reduces the inflammatory response associated with poly(L-lactic acid) fiber. *J. Biomater. Sci. Polym. Ed.* 16:353–370, 2005.
[47]Tsuji, H., M. Ogiwara, S. K. Saha, and T. Sakaki. Enzymatic, alkaline, and autocatalytic degradation of poly (L-lactic acid): effects of biaxial orientation. *Biomacromolecules* 7:380–387, 2006.
[48]Venugopal, J., M. P. Prabhakaran, Y. Zhang, S. Low, A. T. Choon, and S. Ramakrishna. Biomimetic hydroxyapatite-containing composite nanofibrous substrates for bone tissue engineering. *Philos. Transact. A Math. Phys. Eng. Sci.* 368:2065–2081, 2010.
[49]Viljanen, J., H. Pihlajamaki, J. Kinnunen, S. Bondestam, and P. Rokkanen. Comparison of absorbable poly-L-lactide and metallic intramedullary rods in the fixation of femoral shaft osteotomies: an experimental study in rabbits. *J. Orthop. Sci.* 6:160–166, 2001.
[50]Wan, Y., Y. Wang, Z. Liu, X. Qu, B. Han, J. Bei, and S. Wang. Adhesion and proliferation of OCT-1 osteoblast-like cells on micro- and nano-scale topography structured poly(L-lactide). *Biomaterials* 26:4453–4459, 2005.
[51]Yim, E. K., R. M. Reano, S. W. Pang, A. F. Yee, C. S. Chen, and K. W. Leong. Nanopattern-induced changes in morphology and motility of smooth muscle cells. *Biomaterials* 26:5405–5413, 2005.